A route to multiferroics by non-d^0 cation B in magnetic perovskites

To cite this article: Hui Wang and J. G. Che 2011 *EPL* **96** 67012

A Letters Journal Exploring the Frontiers of Physics

December 2011

EPL, **96** (2011) 67012
doi: 10.1209/0295-5075/96/67012

www.epljournal.org

A route to multiferroics by non-d^0 cation B in magnetic perovskites

Hui Wang and J. G. Che[a]

Surface Physics Laboratory (National Key Laboratory), Key Laboratory of Computational Physical Sciences (MOE) and Department of Physics, Fudan University - Shanghai 200433, PRC

received 21 August 2011; accepted in final form 9 November 2011
published online 14 December 2011

PACS 75.85.+t – Magnetoelectric effects, multiferroics
PACS 77.80.-e – Ferroelectricity and antiferroelectricity
PACS 71.15.Mb – Density functional theory, local density approximation, gradient and other corrections

Abstract – Based on first-principles calculations on $BaTcO_3$, we explored a route to promoting ferroelectricity by non-d^0 cation B in magnetic perovskites, leading to the co-existence of magnetic and dielectric ordering in a single phase. The ground state of the perovskite $BaTcO_3$ was found to be an insulator with G-type antiferromagnetic order. A tensile strain in $BaTcO_3$ not only inverted the lowest unoccupied states dominated from t_{2g} to e_g, driving the ferroelectric distortion, but also enlarged this driven force due to the induced narrower gap as its divisor. The tensile strain simultaneously weakened the repulsive force when Tc distorted to one apex of the O-octahedron in $BaTcO_3$. Most importantly, since the physics of our finding is not Tc specific, the route is generally applicable to other magnetic perovskites.

Materials with spontaneous magnetic and dielectric order (magnetoelectric multiferroics) are greatly attractive both for basic physics and for technological applications based on the magnetoelectric effect. However, both ferromagnetism (FM) and ferroelectricity (FE) rarely coexist in nature in a single homogeneous phase [1]. Possible reasons include the so-called d^0 rule [2,3], which states that empty d-shells favor a ferroelectric distortion, but contradict a magnetic ordering associated with partially filled d-shells. In other words, the FE and FM were previously considered to be mutually excluded in a single phase. With the development of synthesis techniques such as thin-film and single-crystal growth methods, layered multiferroic heterostructures can now be artificially grown, see, *e.g.*, refs. [4,5]. Another route to the coupling between FE and FM has been found in some ABO_3 perovskites such as $BiMnO_3$ and $BiFeO_3$. For these materials, the FE can be induced by cation A, while the FM can be driven by cation B [6,7]. The coupling between ferroelectric and magnetic ordering in both the layered multiferroics and the multiferroics induced by two different cations does not break the d^0 rule. However, it is too weak for applications such as the mutual controlling between magnetic and electric ordering, such as inducing a magnetization by means of an electric field and inducing a polarization by means of a magnetic field [1,2,4]. For technological applications, it is crucial to have a strong coupling between electric polarization and magnetization driven by the same cation B in a single phase.

Many efforts have been made to achieve this strong magnetoelectric coupling. Spaldin *et al.* predicted [3] that FE and antiferromagnetism (AFM) could be driven by the same cation Mn in $BaMnO_3$, a non-d^0 B perovskite. They suggested that the d^0 rule could be broken if the competition between the first and second term of the second-order Jahn-Teller effect (SOJT) favored the FE transition, although the d-shell of cation B is partially filled [3]. $CaMnO_3$ and $SrMnO_3$ also belong to this kind of material [8,9]. The FE transition could be driven at the ground state for $BaMnO_3$ while it is promoted under the +1% and +2% strain for $SrMnO_3$ and $CaMnO_3$, respectively [8,9]. The physics behind the controllable factors and the origins favoring the coupling for non-d^0 cation B in ABO_3 perovskites have yet to be identified and explained. On the other hand, most magnetic perovskites are 3d transition metal (TM) based materials. However, 4d TM Tc-based perovskites, $RTcO_3$ (R = Ca, Sr, Ba), were recently found to have G-type antiferromagnetic ordering

[a]E-mail: jgche@fudan.edu.cn (corresponding author)

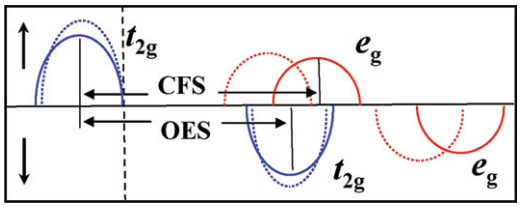

Fig. 1: (Color online) Schematic description for the t_{2g}-e_g order involving on-site exchange splitting (OES) and crystal field splitting (CFS). A tensile strain reduces CFS (dotted lines) but keeps OES unchanged, inverting the lowest unoccupied states from t_{2g} to e_g dominated. The vertical dashed line indicates the Fermi level.

with a high Néel temperature [10–12]. As neighbors of Mn and the lightest radioactive element, the coupling between FE and magnetic ordering in Tc-based perovskites as $R\mathrm{TcO_3}$ ($R =$ Ca, Sr, Ba) is of great interest to physicists.

Based on first-principles calculations on $\mathrm{BaTcO_3}$, we demonstrated in the present work that a tensile strain can always favor a FE distortion in magnetic perovskites. The findings are illustrated in fig. 1. The figure schematically describes an on-site exchange splitting (OES) and a crystal field splitting (CFS) for fivefold-degenerated d orbitals under an O-octahedral field. The Fermi level was found to be at the top of the valence band, indicating its insulating character. A tensile strain reduced the CFS but barely affected the OES, thus inverting the lowest unoccupied states dominated from the spindown t_{2g} to the spinup e_g states and causing the second term of SOJT to favor the FE transition. The tensile strain enhanced the second term because the CFS-reduced gap served as the divisor of the second term. At the same time, the tensile strain weakened the first repulsive term of SOJT due to the enlarged distance between the concerned ions. Because the FE distortion was governed by competition between the two terms of SOJT, we concluded that although the d-shell of the magnetic cation Tc was not zero, but partially filled, a tensile strain may have caused the first and second term of SOJT to favor an off-centering distortion in $\mathrm{BaTcO_3}$.

These results were obtained using the framework of spin density functional theory as implemented in the VASP package [13]. Electron-ion interactions were described by the projector augmented-plane-wave method [14], and the wave functions were expanded in a plane-wave basis set with an energy cutoff of 500 eV. The exchange-correlation potentials were described by the generalized gradient approximation (GGA) in the Perdew-Burke-Ernzerhof form [15]. The k-points in the Brillouin zone (BZ), corresponding to the primitive unit cell with five atoms, were sampled on an $8\times8\times8$ mesh for optimizing structures and a $16\times16\times16$ mesh for calculating density of states. The equilibrium structures were obtained by optimizing atomic positions until the Hellmann-Feynman forces on the atoms were less than 1 meV/Å. Electronic polarizations were determined by calculating Berry's phase [16]. The density functional perturbation theory [17] was used to calculate Born effective charge (BEC), dielectric tensor, and force constants, of which the concerned derivatives were determined by linear response with respect to changes in the ionic positions. For the considered cubic perovskites, a $2\times2\times2$ (40 atoms) supercell was used directly to obtain the phonon frequencies at the specific q-points Γ, R, X, and M. A $3\sqrt{2}\times3\sqrt{2}\times3\sqrt{2}$ (270 atoms) supercell was used to obtain the force constants, which were adopted to construct the dynamical matrix. The complete phonon dispersions were determined by interpolating the dynamical matrix from the q-points in the BZ associated with the supercell to the whole BZ, using the Fourier-interpolation method [18].

To check our calculation setup, the properties of the ground state of $\mathrm{BaTcO_3}$ were calculated and compared with corresponding available data. Franchini *et al.* predicted [11] that the ground state of $\mathrm{BaTcO_3}$ is a G-type AFM insulator under an antiferroelectric distortion (AFD) with $Pnma$ symmetry. In fact, their calculated distortion is quite small, very close to a $Pm\bar{3}m$ cubic with the lattice constant $a = 4.022$ Å. We took the AFD into account by using an initial configuration in the $Pnma$ symmetry with an average Tc-O-Tc angle of approximately 162°. The calculated stable structure indicated that $\mathrm{BaTcO_3}$ tends to be cubic in structure, with the average angle being 179.99° (180° for cubic one) and with a lattice constant of 4.073 Å; the total energy is the same as that of the cubic structure within calculation accuracy. The agreement with the results obtained by Franchini *et al.* [11] is fairly good. Our calculated phonon modes at Γ, M and R points further confirmed the lack of imaginary frequencies associated with the AFD. The slight AFD may be traced to the calculation accuracy: the atomic positions were optimized until the Hellmann-Feynman forces on atoms were less than 1 meV/Å. The ground state of cubic $\mathrm{BaTcO_3}$ was G-type insulating with a local magnetic moment of $1.74\,\mu_B$ at Tc. It was 252, 229, and 131 meV per formula unit lower in energy than that of paramagnetic, ferromagnetism, and C-type AFM, respectively. Therefore, in the following we consider only the G-type AFM structure without AFD.

We now focus on the FE instability in $\mathrm{BaTcO_3}$. A strong coupling between strain and ferroelectricity has been observed. A famous sample was $\mathrm{SrTiO_3}$ [19], whose unstrained state was not ferroelectric at any temperature. However, an epitaxial strain could promote room temperature ferroelectricity and increase its Curie temperature by hundreds of degrees. In order to determine the strain effects on instabilities in $\mathrm{BaTcO_3}$, we introduced an isotropic strain to the $\mathrm{BaTcO_3}$ with G-type AFM and calculated the phonon frequencies at the Γ point as a function of an isotropic strain defined as $(a-a_0)/a_0$, where a_0 denotes the lattice constant of the cubic perovskite. In fig. 2 we show the variation of the phonon frequencies with the strain for two kinds of polar vibration modes, which are indicated by arrows. The figure clearly shows

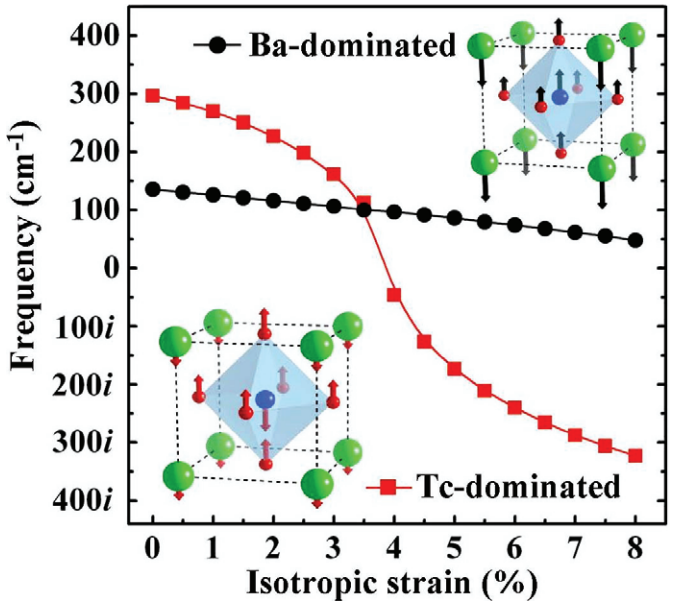

Fig. 2: (Color online) Phonon frequencies for the strained $BaTcO_3$ at the Γ point as a function of strain. Frequencies below zero ($i\,\mathrm{cm}^{-1}$) for unstable phonons. Squares and circles represent the frequencies of the Tc- and Ba-dominated vibrational modes, which are indicated by the bottom left and the top right inset, respectively.

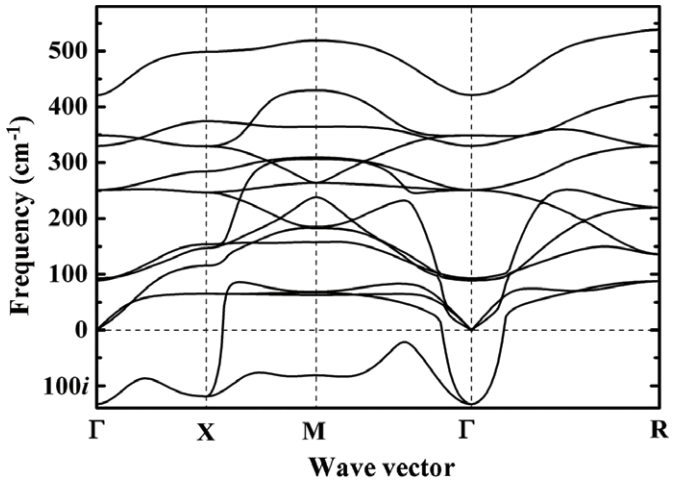

Fig. 3: Phonon frequencies for the +4.5% strained $BaTcO_3$ along the high-symmetry axis in BZ. Frequencies below zero ($i\,\mathrm{cm}^{-1}$) for unstable phonons.

that the Tc-dominated mode was strongly sensitive to the isotropic strain and softened to imaginary frequency from the beginning of +4% strain, while the Ba-dominated mode remained stable up to +8% isotropic strain.

In order to identify the unstable vibrational modes, the phonon dispersion of $BaTcO_3$ under the +4.5% isotropic strain was calculated and depicted in fig. 3. In the calculations, the LO-TO splitting was taken into account by using the calculated BECs (Tc = 7.36, Ba = 2.76, $O_{\parallel} = -6.64$, $O_{\perp} = -1.74$, in e) and optical dielectric constant (13.12) for the +4.5% strained $BaTcO_3$. As shown in fig. 3, the

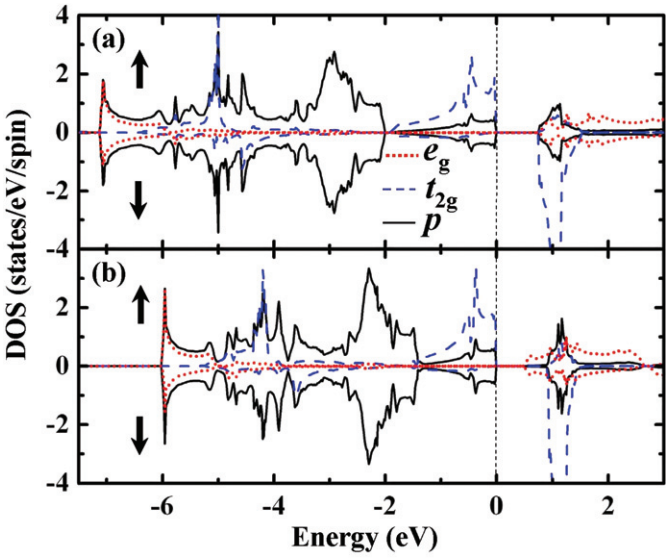

Fig. 4: (Color online) Orbital-resolved density of states of t_{2g}, e_g and p for the unstrained $BaTcO_3$ (a) and the +4.5% strained $BaTcO_3$ (b). The lowest unoccupied states turn from the t_{2g} dominated in (a) to the e_g dominated in (b) with a change of the energy gap from 0.72 in (a) to 0.48 eV in (b). The Fermi energy is set at zero.

only unstable mode with a frequency of $127\,i\,\mathrm{cm}^{-1}$ at the Γ point was the Tc-dominated polar mode associated with Tc displacement towards one apex of the O-octahedron. This mode, which was unstable along Γ-X-M-Γ direction, increased sharply from the Γ to the R point, indicating a chainlike unstable localized distortion found also for phonons in $BaTiO_3$ [20], a typical ferroelectric perovskite. Therefore, a ferroelectric phase likely exists at this volume with a calculated polarization of $30.7\,\mu\mathrm{C/cm}^2$. From fig. 3, we could not find any imaginary frequency associated with AFD at the BZ boundary, implying that a rotation distortion of the O-octahedron probably did not occur in the +4.5% strained $BaTcO_3$. Based on the LDA+U method, Rondinelli *et al.* considered the correlation effects on the non-d^0 Mn-driven ferroelectricity in $BaMnO_3$ and verified that the phonon modes are robust to the effects [3]. Hence, the correlation effects were not taken into account in the present work.

In order to capture the physics behind the FE transition in $BaTcO_3$ with a strain as great as +4%, we calculated orbital-resolved density of states (DOS) of the unstrained and the +4.5% strained $BaTcO_3$ and plotted them in figs. 4(a) and (b), respectively. Both the unstrained and the strained $BaTcO_3$ were insulators. For spinup electrons, t_{2g} states mixed with some O p states were fully occupied by the three remaining d electrons of Tc^{+4}, leaving the e_g states empty with an energy gap. For spindown electrons, the d states (t_{2g} and e_g) were fully separated from the O p-bands due to the on-site exchange interactions of Tc and were shifted up above the Fermi level. Furthermore, because of less hybridization with the O p states, the t_{2g} states for spindown electrons were much narrower and

sharper compared with those of the occupied t_{2g} states for spinup electrons (fig. 4).

The striking difference in DOS between the unstrained and strained $BaTcO_3$ involving our topic was the energy order of the t_{2g} and e_g in the unoccupied states: for unstrained $BaTcO_3$, the lowest unoccupied states were the t_{2g} of spindown electrons dominated. However, for the +4.5% strained $BaTcO_3$, the lowest unoccupied states turned from the t_{2g} to the e_g of spinup electrons dominated. Similar electronic features were found for $BaMnO_3$ [3], a typical perovskite with both the ferroelectricity and magnetism driven by the same non-d^0 cation (Mn) on the perovskite site B. This difference was mainly induced by e_g low-shifting, which is understandable [21] given that the O-octahedral crystal field was weakened by +4.5% tensile strain (fig. 1), while the energy position of t_{2g} was largely unchanged (change less than 0.03 eV). Thus, the energy gap was reduced from 0.72 eV for unstrained to 0.48 eV for the +4.5% strained $BaTcO_3$.

The strain-induced change in the energy order of the t_{2g}-e_g and in the energy gap are crucial for the FE transition in $BaTcO_3$. Keeping these two facts in mind, the FE transition of the strained $BaTcO_3$ can be now understood. Rondinelli *et al.*, in analyzing the FE transition of $BaMnO_3$, suggested that the competition between the first and the second term of SOJT would determine the stability of an off-centering of cation B in a perovskite [3]. We found that the contribution of the second term to the FE transition was mainly governed by the energy gap and the orbital parity. The hybridization may not have contribution to the second term of SOJT due to the orbital parity. On the other hand, the second term was inversely proportional to the energy gap between the lowest unoccupied states and the topmost occupied states: the smaller the gap, the larger the second term. Therefore, the tensile strain favored the FE distortion due to the second term of SOJT in two ways: first, it led to the inversion of the lowest unoccupied states dominated by e_g, resulting in a nonzero contribution to the second term; second, it enhanced this contribution by reducing the gap to a smaller divisor in the second term.

As discussed above, the condition of the FE distortion was e_g low-lying for nonzero contribution to the second term of SOJT. $BaMnO_3$ satisfies the condition in the ground state [3]. In contrast, $BaTcO_3$, a perovskite similar to $BaMnO_3$, with Mn replaced by Tc, needed to apply a tensile strain as large as +4% for the FE transition. The reason may be traced to different behaviors of $3d$ (Mn) and $4d$ (Tc) electrons of non-d^0 cation on the perovskite B site. Owing to more delocalization, the exchange splitting of $4d$ electrons was smaller than that of $3d$ electrons [22]. The unoccupied $4d$ t_{2g} states of spindown electron could not be shifted up over the unoccupied e_g states of spinup electron, as shown in fig. 1. This situation could be changed by applying a tensile strain; increasing the O-Tc distance could effectively decrease its CFS under the O-octahedral field, thereby low-shifting the e_g states of spinup states, while the OES would remain nearly unchanged. The reduction of the CFS by the tensile strain compensated for the shortage of the small OES of $4d$ electrons and favored the FE transition in $BaTcO_3$. This argument can be also used to explain why $SrMnO_3$ and $CaMnO_3$ could be ferroelectric with a tensile strain as large as +1% and +2% [8]. The reason may be the same: the atomic radius of Sr and Ca were smaller than that of Ba, leading to the smaller lattice constants of $a_0 = 3.67$ and 3.845 Å [8,9], respectively. Increasing their lattice parameters artificially stabilizes their FE phase.

The first term of SOJT, a short-range repulsive term between the displaced cation B and oxygen, is a dominantly unfavorable factor for the FE transition. The smaller the first term, the more favorable the FE transition. Therefore, it does also favor the FE transition for $BaTcO_3$ under the tensile strain, since increasing the Tc-O distance due to the tensile strain directly reduces the first term of SOJT.

In order to support the argument about the role of two terms of SOJT in the FE transition, we decomposed the first and second term of SOJT from a double-well potential of an isotropic strained $BaTcO_3$. We then recombined them to a double-well potential of a biaxial strained $BaTcO_3$ and compared it with the directly calculated corresponding one. We first calculated the total energy variations as a function of Tc off-centering in the unstrained $BaTcO_3$. Assuming that the energy variation was induced only by the first term, we fit it to the Lennard-Jones potential (L-J), p/r^{12}. The fitted parameter was obtained as $p = 933.81493\,\text{eV}\text{Å}^{12}$. We note here that in this fitting process, only one parameter was used to fit the energy change with the Tc-displacement (11 points ranging from 1.96–2.04 Å). The maximum error was as small as 0.15 meV, implying that our assumption about the energy change in the L-J type associated with the repulsive term was fairly reasonable.

Then we calculated the double-well potential for the +8% isotropic strained $BaTcO_3$, from which we decomposed the second term by reducing the fitted L-J potential. Then, for a +8% biaxial strained $BaTcO_3$ with the third axis unstrained, the double-well potential was recombined using the L-J potential and the decomposed second term with a 2/3 factor. The 2/3 factor assumed that the e_g orbitals were equivalent in the xyz directions. The results are plotted as a solid curve in fig. 5. By comparison, the directly calculated corresponding double-well potential is shown as circles in the same figure. The agreement between the recombined and the directly calculated double-well potential in both the depth and the position of the lowest potential indicates that the second term of SOJT, which led the nonzero contribution to favor the FE transition, was governed by whether or not the lowest unoccupied states were e_g dominated.

In summary, based on first-principles calculations, we demonstrated that the ground state of cubic $BaTcO_3$ was a G-type AFM insulator with a local magnetic moment

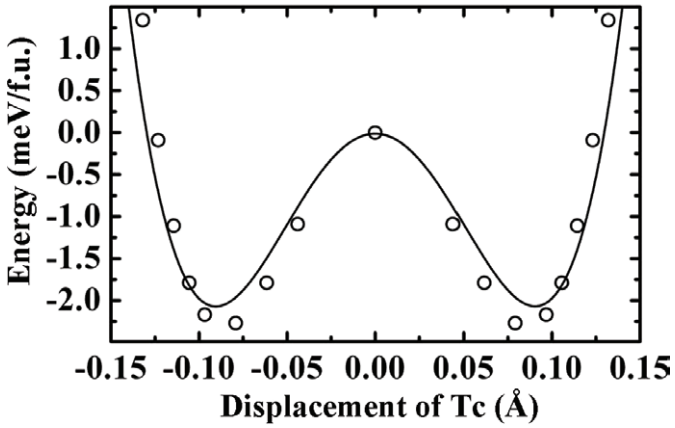

Fig. 5: Comparison between the model and the direct calculated double-well potential. The solid line and circles were obtained by the model and the direct calculations, respectively.

of $1.74\,\mu_B$ at Tc. There were no imaginary frequencies associated with AFD. The calculated results showed that the phonon and electronic properties of $BaTcO_3$ were strongly sensitive to strain. A tensile strain in $BaTcO_3$ may induce the FE instability because a tensile strain can invert the lowest unoccupied state character from t_{2g} to e_g and reduce the repulsive forces between Tc and O, resulting in two deciding factors of SOJT favoring the phase transition. The numerical experiment for the double-well potential confirmed the key contribution of two terms of SOJT on the FE transition under a tensile strain. Therefore, our finding prescribes a way to break the d^0 rule and to induce the ferroelectric and magnetic order by the same cation on the perovskite B site. Most importantly, we emphasize that this conclusion may be valid for other perovskites with the features shown in fig. 1, since that figure is not specifically associated with Tc.

* * *

This work was supported by the NFSC, MOE, MOST of China (No. 2009CB929204 and 2011CB921803).

REFERENCES

[1] See, *e.g.*, Spaldin N. A., Cheong S. W. and Ramesh R., *Phys. Today*, **63**, issue No. 10 (2010) 38.
[2] Hill N. A., *J. Phys. Chem. B*, **104** (2000) 6694.
[3] Rondinelli J. M., Eidelson A. S. and Spaldin N. A., *Phys. Rev. B*, **79** (2009) 205119.
[4] Fiebig M., *J. Phys. D: Appl. Phys.*, **38** (2005) R123.
[5] Tokura Y., *J. Magn. & Magn. Mater.*, **310** (2007) 1145.
[6] Seshadri R. and Hill N. A., *Chem. Mater.*, **13** (2001) 2892.
[7] Wang J., Neaton J. B., Zheng H., Nagarajan V., Ogale S. B., Liu B., Viehland D., Vaithyanathan V., Schlom D. G., Waghmare U. V., Spaldin N. A., Rabe K. M., Wuttig M. and Ramesh R., *Science*, **299** (2003) 1719.
[8] Bhattacharjee S., Bousquet E. and Ghosez P., *Phys. Rev. Lett.*, **102** (2009) 117602.
[9] Lee J. H. and Rabe K. M., *Phys. Rev. Lett.*, **104** (2010) 207204.
[10] Rodriguez E. E., Poineau F., Llobet A., Kennedy B. J., Avdeev M., Thorogood G. J., Carter M. L., Seshadri R., Singh D. J. and Cheetham A. K., *Phys. Rev. Lett.*, **106** (2011) 067201.
[11] Franchini C., Archer T., He J., Chen X. Q., Filippetti A. and Sanvito S., *Phys. Rev. B*, **83** (2011) 220402.
[12] Heyd J., Scuseria G. E. and Ernzerhof M., *J. Chem. Phys.*, **118** (2003) 8207; **124** (2006) 219906(E).
[13] Kresse G. and Hafner J., *Phys. Rev. B*, **47** (1993) 558; **49** (1994) 14251; Kresse G. and Furthmüller J., *Comput. Mater. Sci.*, **6** (1996) 15; *Phys. Rev. B*, **54** (1996) 11169.
[14] Blöchl P. E., *Phys. Rev. B*, **50** (1994) 17953.
[15] Perdew J. P., Burke K. and Ernzerhof M., *Phys. Rev. Lett.*, **77** (1996) 3865.
[16] King-Smith R. D. and Vanderbilt D., *Phys. Rev. B*, **47** (1993) 1651; Vanderbilt D. and King-Smith R. D., *Phys. Rev. B*, **48** (1993) 4442.
[17] Wu X. F., Vanderbilt D. and Hamann D. R., *Phys. Rev. B*, **72** (2005) 035105.
[18] Gonze X. and Lee C., *Phys. Rev. B*, **55** (1997) 10355; Wang H., Wang Y. F., Cao X. W., Feng M. and Lan G. X., *J. Raman Spectrosc.*, **40** (2009) 1791; Togo A., Oba F. and Tanaka I., *Phys. Rev. B*, **78** (2008) 134106.
[19] Haeni J. H., Irvin P., Chang W., Uecker R., Reiche P., Li Y. L., Choudhury S., Tian W., Hawley M. E., Craigo B., Tagantsev A. K., Pan X. Q., Streiffer S. K., Chen L. Q., Kirchoefer S. W., Levy J. and Schlom D. G., *Nature*, **430** (2004) 758.
[20] Ghosez P., Cockayne E., Waghmare U. V. and Rabe K. M., *Phys. Rev. B*, **60** (1999) 836.
[21] Hong F. and Che J. G., *Phys. Rev. Lett.*, **96** (2006) 167206.
[22] Sarma D. D., Mahadevan P., Saha-Dasgupta T., Ray S. and Kumar A., *Phys. Rev. Lett.*, **85** (2000) 2549.